Zhang *et al. Microstructures* 2024;4:2024041
DOI: 10.20517/microstructures.2024.03

Microstructures

Review

Open Access

Check for updates

Recent progress of operando transmission electron microscopy in heterogeneous catalysis

Fan Zhang[1,2], Wei Liu[1,2]

[1]State Key Laboratory of Catalysis, iChEM, Dalian Institute of Chemical Physics (DICP), Chinese Academy of Sciences, Dalian 116023, Liaoning, China.
[2]University of Chinese Academy of Sciences, Beijing 101408, China.

Correspondence to: Prof. Wei Liu, State Key Laboratory of Catalysis, iChEM, Dalian Institute of Chemical Physics (DICP), Chinese Academy of Sciences, Dalian, Liaoning 116023, China. E-mail: weiliu@dicp.ac.cn

How to cite this article: Zhang F, Liu W. Recent progress of operando transmission electron microscopy in heterogeneous catalysis. *Microstructures* 2024;4:2024041. https://dx.doi.org/10.20517/microstructures.2024.03

Received: 10 Jan 2024 **First Decision:** 22 Mar 2024 **Revised:** 9 Apr 2024 **Accepted:** 22 May 2024 **Published:** 9 Jul 2024

Academic Editor: Zibin Chen **Copy Editor:** Fangyuan Liu **Production Editor:** Fangyuan Liu

Abstract

As a highly intricate process encompassing multiple length scales, catalysis research evolves into a comprehensive understanding of reaction kinetics across microscopic to atomic dimensions when electron microscopy, particularly the *in situ* transmission electron microscopy (TEM), emerges to be increasingly relevant. Meanwhile, the absence of effective methodologies for measuring reaction products during catalysis complicates efforts to elucidate the operational state and catalytic activity of the catalyst. With ongoing advancements of refined gas-cell design within TEM and other *in situ* accessories, diverse methodologies have emerged to ascertain the occurrence of chemical reactions. In this review, we summarized the recent progress of operando TEM while further extending its conceptual boundaries by including newly emerged reaction-detecting approaches capable of bridging microstructure to the reaction process. These methods involve not only traditional ones of product detection, e.g., *in situ* mass spectrometry and electron energy loss spectroscopy, but also other reaction-correlative characterizations, such as directly imaging reactant molecule, modified *in situ* reactor for thermogravimetry and temperature-programmed reaction, and TEM image-based microstructure quantification and activity correlation. Applications, inherent challenges, and our perspectives within these operando TEM techniques are deliberated.

Keywords: Operando TEM, structure-activity relationship, heterogeneous catalysis, molecules detection, thermogravimetry

INTRODUCTION

Catalysis plays a pivotal role in contemporary industries, with approximately 85% of chemical products manufactured through catalytic processes[1,2]. Particularly in a typical gas-solid catalytic reaction, substrate molecules diffuse from the gas phase and adsorb onto the surface of solid catalysts. Adsorbed molecules undergo chemical bond cleavage and recombination on the catalyst surface, generating products. Only the atoms at the active sites of the catalyst surface/interface can interact with the substrate molecules and participate in reactions. The performance of a catalyst is predominantly governed by its microstructure, particle size, morphology, composition, and metal-support interactions[3-5].

To put insights into the status of a working solid catalyst, *in situ* characterizations, represented by infrared spectroscopy (IR) and Raman spectroscopy, can detect surface functional groups on the catalyst during the reaction process by analyzing the positions of absorption peaks. They can determine the changes in aspects of surface composition and microstructure, aiding in the speculation of catalytic reaction intermediates and further revealing the catalytic mechanism[6,7]. Besides, X-ray absorption spectroscopy (XAS) provides local structural and electronic information about materials, making it one of the most suitable analytical techniques for studying the geometry, oxidation state, and even electronic structure of nanoclusters[8]. To date, a large variety of *in situ* spectroscopy techniques have elucidated versatile dynamic evolutions of heterogeneous catalysis under reaction conditions[9-12]. These metastable, high-energy structures can only be collected under reaction conditions in synergized measurement of the chemical reactions. The macroscale region of these spectroscopic studies makes them inefficient in revealing the true active sites normally in the atomic range. Therefore, elucidating the dynamic behavior of the catalyst and discerning its intrinsic activity hold paramount significance. Microscopy studies, especially the *in situ* (scanning) transmission electron microscopy (S/TEM), play an increasingly important role in unveiling the activity origin and reaction kinetics at both microscopic and atomic scales[13-15]. However, the catalyst undergoes diverse structural states during the initial, intermediate, and final stages of a reaction, leading to sophisticated scenarios when linking these evolving microstructures to reaction performance[16,17]. Consequently, directly correlating reaction performance with the catalyst's microstructure in real time, under an identical environment, at the same sample location is imperative for advancing the catalyst design.

In situ electron microscopy technology has been developed with combined environment loading and dynamic imaging technology based on the high spatial resolution of electron microscopy, enabling online *in situ* microscopic analysis of materials with high spatiotemporal resolution in a controlled environment. Its pervasive applications extend across multiple materials-related research disciplines, notably in energy chemistry and semiconductor physics, where it increasingly contributes to seminal scientific discoveries[18-20]. Although *in situ* electron microscopy adeptly reveals structural and chemical composition alterations of catalysts under reaction atmosphere conditions, it falls short of detecting the actual occurrence of catalytic reactions. The gap between the reaction circumstances of *in situ* electron microscopy and practical reactors poses formidable challenges to unambiguously establishing precise and reliable connections of catalyst restructuring and activity. This, unfortunately, leads to the indirect attribution or even conjectures about the active sites and reaction mechanisms simply according to the observed structural transformations. To address this inherent limitation, it is imperative to develop a methodological framework capable of concurrently quantifying catalytic product formation while monitoring the catalyst's structure and composition. Furthermore, it necessitates the electron microscopy characterization from the confines of *in situ* environments to operando scenarios, thereby affording in-depth insights into the microscale dynamics of catalytic processes[21,22].

The term "operando", which originates from the *Raman* spectroscopy domain, refers to the capability of simultaneously detecting both structure and catalytic activity. This approach not only facilitates the determination of reaction kinetics but also contributes to establishing structure-activity relationships[23]. Particularly in a typical technique of operando TEM, it refers to the direct detection of catalytic activity alongside the observation of structural transformations in the catalyst. Advanced by recent developments of low-dose imaging and integrated Micro-Electro-Mechanical System (MEMS) chip technique, refined strategies have emerged to ascertain the occurrence of chemical reactions within the TEM reactor and to unravel the elaborate structure-activity relationship, specifically discerning the active sites under operational conditions. As shown in Figure 1, multiphase catalytic processes involve the adsorption, reaction, and desorption of gas molecules at active sites on solid catalyst surfaces. Achieving visualization of the adsorption of reactant molecules on the catalyst surface and their reaction processes at the atomic level can provide the most direct evidence for chemical reactions in an electron microscope [Figure 1A]. Modification of MEMS chips integrating micro-cantilever technology enables the correlation of microstructural evolution with spectroscopic characterizations such as reaction-induced thermogravimetric analysis (TGA) and hydrogen temperature-programmed reduction (H_2-TPR) [Figure 1B]. Trace product gases can be detected using TEM-optimized mass spectrometers or electron energy loss spectroscopy (EELS) with local gas detection capabilities, facilitating direct detection of catalytic activity [Figure 1C]. Quantitative structural information extracted through deep learning-based high-throughput analysis of microscopy data enables the correlation of microstructural details with macroscopic performance [Figure 1D].

This review broadens the conceptual boundary of operando TEM, aiming to enrich the solution alternatives of direct identification upon microstructure origin for specific reaction activity under operational conditions. Section "MEANS FOR DETECTING CATALYTIC PRODUCTS IN OPERANDO TEM" outlines various advanced technologies employed in operando TEM, encompassing diverse methodologies, as shown in Figure 1. Section "OPERANDO TEM PRACTICAL APPLICATION" offers a detailed survey of the latest research focused on achieving a more profound understanding of catalysis through operando TEM. The concluding section of this review discourses the challenges and prospective developments in operando TEM technology.

MEANS FOR DETECTING CATALYTIC PRODUCTS IN OPERANDO TEM

Direct detection of catalytic products

Conventional electron microscopes are usually operated within a high vacuum environment, serving a dual purpose. Firstly, this practice is implemented to preserve the integrity of the electron emitter and prevent electron scattering of gas, thereby upholding spatial resolution. Secondly, it aims to mitigate sample contamination from residual hydrocarbons in the electron microscope atmosphere. Consequently, maintaining optimal vacuum conditions is imperative to guarantee the electron microscope performance. However, this inherent necessity poses a challenge when investigating materials within operational contexts, such as reaction atmospheres or liquid environments. To address this inherent contradiction, Marton from the University of Brussels in Belgium proposed two methods in 1935 to manipulate gas pressure and composition within an electron microscope[24]. These methods facilitate the imaging of wet samples while minimizing potential damage to biological specimens and contamination within the electron microscope.

The first method involves modifying the specimen holder to include a pair of electron-transparent windows positioned above and below the sample, effectively sealing the sample and the gas atmosphere. This modification isolates the sample from the electron microscope chamber, thereby preventing gas ingress into the vacuum system of a TEM chamber. This technique, referred to as the "closed cell", is now recognized as

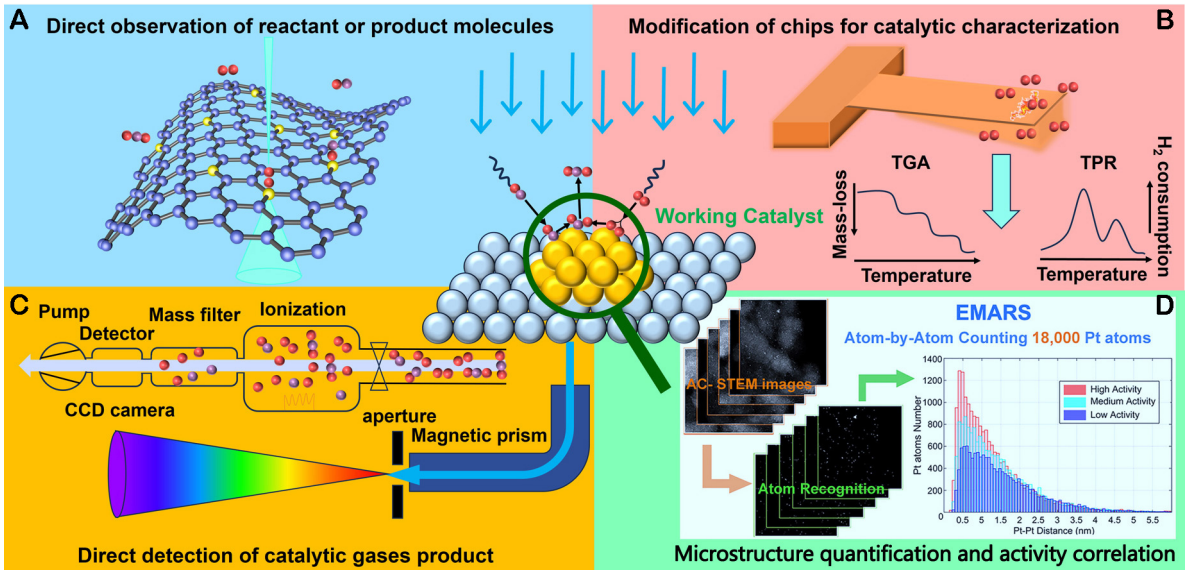

Figure 1. Schematic outlining various advanced technologies employed in operando TEM. (A) Direct observation of reactant or product molecules. (B) Chip modification for catalytic reactions. (C) Direct detection of catalytic products. (D) TEM image-based microstructure quantification and activity correlation.

gas cell technology. The second strategy involves altering the objective pole components of the electron microscope. Introducing a pair of apertures above and below the specimen restricts the release of gas into the chamber near the specimen. A differential pump system facilitates the controlled evacuation of gas through small apertures, thereby maintaining a pressure differential between the sample area and the rest of the TEM chamber. This differential pumping approach is contemporarily identified as Environmental Transmission Electron Microscopy (ETEM) technology. These two methods, embedding with TEM to present, have successfully enabled the study of material behavior *in situ* within a controlled environment while concurrently preserving the vacuum conditions of the entire microscope. To date, these methodologies have undergone continued technique promotion and gained widespread utilization[25,26].

The "Gas Cell" technology employs a specialized specimen holder, coupled with a window unit, to introduce gases or liquids into a pair of sealed membranes without compromising the high vacuum conditions within the electron microscope chamber and the electron gun. As depicted in Figure 2A, the modern *in situ* TEM gas cell consists of two matching silicon chips, each containing a central hole of 1 mm^2 and covered by a 1.2 μm thick membrane of Si_3N_4. This Si_3N_4 membrane is etched at the center to create the amorphous Si_3N_4 window with a thickness of 10 nm [Figure 2B]. The opposing membranes of the top and bottom form the shallow gas-flow channel [Figure 2C][27]. This design ensures the containment of gases at one atmosphere or higher air pressure, depending upon the strength and thickness of the window. The system is linked to the specimen holder through a dedicated gas supply system. Diverse gases, drawn from separate gas bottles, undergo mixing within the gas system. The inlet and outlet pressures are accurately controlled by two pressure controllers to achieve a consistent and stable gas flow with regulated pressure and flow rates[28]. The "gas cell" technology has been successfully commercialized since the 2010s; two representative providers are DENssolutions and Protochips companies. Nowadays, the "gas cell", due to its compatibility with conventional TEM and its minimal requirement of a specimen holder and gas supply system, has been widely adopted, emerging as a commonly technical solution in the realm of *in situ* atmospheric electron microscopy. This technology processes advances of the facile integration of a mass spectrometer at the rear end of the specimen holder for detecting gaseous products, thereby affording the

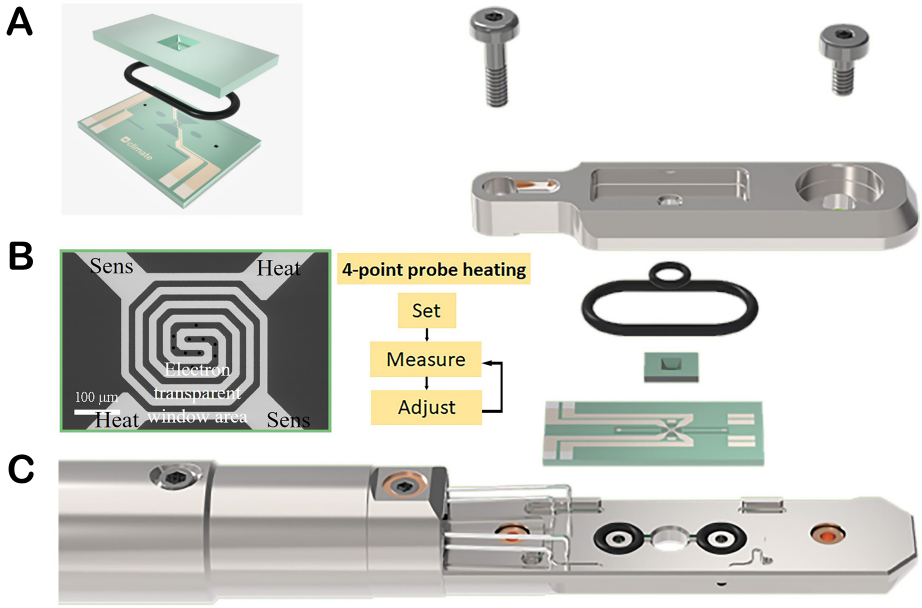

Figure 2. Structural ensemble of MEMS chips fitting to the specialized TEM holder. (A) The upper and lower MEMS chips and rubber O-ring. (B) SEM image of the SiN_x window on MEMS chip and the temperature control method. (C) Side view of a modern MEMS-based *in situ* TEM holder. Example from DENSsolutions[27].

measurement of conversion rates and catalyst activity, as exemplified in Figure 3A[29,30]. However, a challenge remains, which lies in the limited capacity of the reactor to carry catalysts. Consequently, too small a quantity of product gas results in insufficient detection of mass spectrometers.

In traditional mass spectrometry operations, it is customary to redirect the gas from the primary circuit to the branch circuit, wherein a portion of the gas undergoes ionization before entering the detection chamber[31]. This configuration necessitates a substantial gas flow and constrains the flexibility of controlling the pressure and flow rate inside the gas cell. To address this limitation, the mass spectrometer pipeline was optimized in the context of operando TEM, as delineated in Figure 3B. Notably, a molecular pump was strategically positioned behind the detection chamber, and the volume of gas entering the chamber was regulated via a needle valve to enhance the sensitivity of the mass spectrometer to trace quantities of product gases. The surplus gases were subsequently channeled back into the gas supply system following their passage through the spectrometer, ensuring the stability of pressure and flow rates within the reactor[32,33].

This operando TEM configuration facilitates comprehensive analysis of all gas products within the reactor through the mass spectrometer. The modest quantity of catalyst required for inducing detectable changes in gas products ensures a responsive outcome in the mass spectrometer. However, due to the constraint associated with the limited number of catalysts, only reactions characterized by high conversion rates (such as H_2/O_2, CO/O_2, CH_4/O_2, CO_2/H_2) currently permit the simultaneous measurement of structure and performance within operando TEM. Another critical constraint in evaluating catalytic activity lies in the time delay between the measurement positions of various parameters in the operando TEM setup. Calibration of these time delays before experimentation is imperative for securing accurate data correlation; otherwise, erroneous results may ensue[28,30]. Factors influencing time delay inside the gas cell involve the gas flow rate, gas pressure, and the length of the connecting pipeline. While the length of the connecting pipe

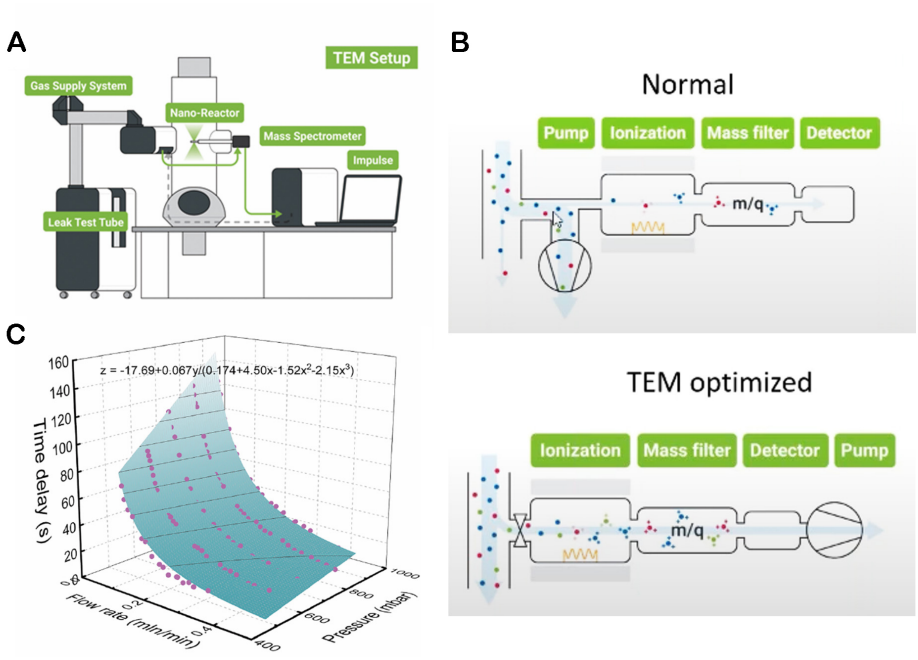

Figure 3. (A) The schematic view of a gas cell-based operando TEM gas path. (B) The working principle and gas path schematic view of traditional MS and TEM optimized MS[32], CO pink, O_2 green, He blue. (C) The delay time variation with Nano-Reactor gas flow rate and pressure. (A and C) have been reproduced from ref.[33]. Copyright 2022, Elsevier.

typically remains constant throughout an experiment, it is advisable to employ the shortest possible connection to minimize dead volume and reduce time delays. A readily available open-source script facilitates automated measurement and calibration of time delays based on the functional relationship between the time delay, gas flow rate, and gas pressure [Figure 3C], expediting effective data synchronization and ensuring more dependable information association[33].

The ETEM technique employs positioned apertures, both above and below the specimen, to permit the passage of incident, diffracted, and scattered electron beams while concurrently restricting the flow of gas in proximity to the specimen into the chamber. A multi-stage turbomolecular pump system is then utilized to exhaust the gas leaking from the apertures out of the system. The coordinated control of aperture size and the differential pump ensures that the specimen chamber maintains a specified pressure condition, thereby preserving a high vacuum environment near the electron source and electron path. This approach safeguards against strong electron scattering and gas dispersion in the chamber, thereby preventing a reduction in imaging resolution. Notably, the maximum gas pressure is confined to 20 mbar in ETEM. Compared to the gas-cell approach, ETEM does not involve windowed reactors with layer films, thereby reducing electron beam scattering and thus preserving the fundamental instrument resolution. Additionally, it also eliminates the potential risks of gas leakage associated with film rupture during gas flow, mitigating the likelihood of damage to the electron microscope, especially the electron gun, during *in situ* atmospheric experiments. Currently, ETEM equipped with image aberration-correctors has been widely employed in *in situ* atmospheric and heating experiments, with the ETEM produced by Thermo Fisher Scientific being a representative example. To further observe and investigate the dynamic behaviors of single atoms and small clusters, companies such as Hitachi have also introduced probe aberration-corrected microscopes, namely environmental STEM (ESTEM) systems.

ETEM enables the controlled introduction of various gas combinations through a gas mixing tank and a fine valve (leak valve) [Figure 4A][34]. The composition of the gas can be ascertained through the inclusion of a residual gas analyzer (RGA) within the system. However, due to spatial constraints in ETEM and the necessity to avoid interference with electron optical properties, the RGA is typically positioned at a considerable distance from the specimen. Additionally, drawbacks exist to compromise the signal-to-noise ratio for gas product detection, including the significantly lowered pressure in ETEM compared to the working pressure of the catalyst and the considerable dead volume of the TEM chamber relative to the amount of catalyst loading. These limitations present a substantial challenge in detecting catalytic products and ascertaining catalytic activity in the operando ETEM setup.

Electron Energy Loss Spectroscopy (EELS) has been proven to be a successful tool for detecting local gas composition due to its elemental identification capability and high spatial resolution. Notably, Crozier *et al.* achieved a milestone by successfully detecting N_2, H_2, CO, and CO_2, among other mixtures in ETEM[35]. This methodology entails acquiring a reference spectrum for each individual gas under identical optical conditions and known pressures as those employed in the experiment. The gas composition is subsequently determined through linear fitting of the spectrum of the mixed gas against the individual gas spectra[35]. This *in situ* EELS approach allows for real-time analysis of gas components within the reaction cell and facilitates swift measurements with acquisition times of a few seconds. Consequently, EELS has emerged as a potent tool for realizing operando TEM. This method has been employed to quantitatively measure reaction products and assess the activity in CO oxidation and CO_2 methanation on Ru-based catalysts in ETEM [Figure 4B], thereby achieving the simultaneous detection of catalyst structure and catalytic activity[34].

Beyond local gaseous environment measurements, an alternative approach involves increasing the catalyst loading within the ETEM to yield more gas products for stronger gas product signals. This enables accurate quantification of catalyst activity using existing accessories such as RGA or EELS integrated with ETEM. As depicted in Figure 4C and D, Miller *et al.* sintered broken glass fibers into a hollow disc carrier with a diameter of 3 mm and a thickness of 0.6 mm[36]. The surface area of this carrier is 7 cm^2, which is 50 times the surface area of a standard 200 mesh 3 mm TEM carrier grid. Upon dropping the catalyst suspension onto the disc carrier and subsequent drying, it can be secured into a crucible-type heating holder. This approach indicates that a substantial quantity of catalysts is available using the glass fiber carrier, significantly improving the catalytic conversion rate in ETEM. Both RGA and EELS were effectively employed to analyze gas components. This methodology allowed for the study of the structure-activity relationship in the CO oxidation reaction on Ru nanoparticle catalysts, enabling real-time observation of catalyst structure and reaction performance at the atomic level[36,37].

Direct observation of reactant or product molecules

One intuitive approach to depict a reaction is directly observing interacted reactant molecules at the atomic level. Visualizing the adsorption sites and reaction processes on the catalyst surface in real time can furnish the most immediate evidence for verifying active sites, comprehending the catalytic mechanism, and establishing the catalyst structure-activity relationship under operational conditions to facilitate operando TEM. It presents significant challenges to directly observe gas molecules in TEM, particularly those randomly adsorbed on the catalyst surface. Image Contrast of these molecules manifests as a uniform background in the image, lacking sufficient visibility and exhibiting heightened sensitivity to electron beams, making it challenging to discern individual adsorption sites. As one representative, Yuan *et al.* proposed a method to organize randomly distributed vapor molecules on an orderly arranged, clean TiO_2 (001) surface[38]. Specifically, Ti_{4c} atomic columns protrude from the atomically flat TiO_2 surface, aligning parallel to the incident electron beam. Importantly, these Ti_{4c} sites function as active sites for H_2O adsorption and dissociation. The resulting contrast from the orderly superimposed double protrusion

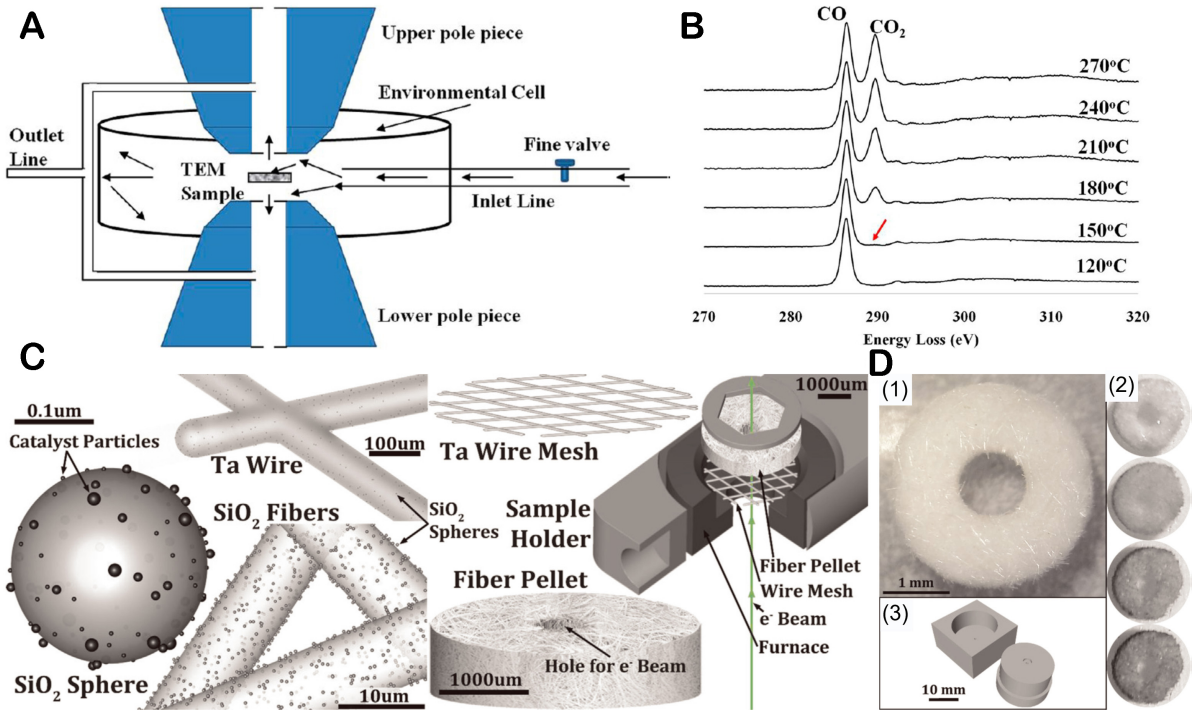

Figure 4. (A) The schematic view of ETEM reactor. (B) Background subtracted EELS acquired at different temperatures during CO oxidation on Ru/SiO_2 catalyst in an ETEM reactor. Reprinted with permission from ref.[34] Copyright 2012, American Chemical Society. (C) The schematic view of optimized operando TEM sample. (D) The images of operando pellet (1) and the pellet after drops of catalyst suspension have dried (2). (3) The jig designed to finish the pellets. (C and D) have been reproduced from ref.[36].Copyright 2015, Elsevier.

structures significantly enhances the imaging contrast of gas molecules, enabling the direct observation of reactant gas molecules and their adsorption sites, as depicted in Figure 5A. Subsequently, introducing CO, another gas reactant, into the ETEM destabilizes the previously stable double protrusion structure under water vapor conditions [Figure 5B]. The dynamic change, in contrast, indicates the interaction between adsorbed water groups and CO molecules, confirming the water-gas shift reaction in ETEM. This approach elucidates the reaction's active sites under working conditions and contributes to establishing the catalyst structure-activity relationship[19].

TEM technology offers rapid imaging speed (over 1,000 frames/s or one millisecond/frame of 4,096 × 4,096 pixels) and is sensitive to single-electron events as for typical direct detection characteristics (total dose for a TEM image < 10 e·Å^{-2}), yet its imaging capabilities are constrained by the contrast transfer function, and the image contrast undergoes reversal with changes in sample thickness. This complexity, especially in identifying adsorbed gas molecules, induces increasing challenges of image interpretation. In contrast, positively correlated with atomic number, the intuitive contrast of STEM mode facilitates easier image interpretation. Particularly upon the emergence of differential phase contrast techniques (DPC), which utilizes segmented annular detectors to collect low-angle scattered electrons at much lowered electron dose. By measuring the center of mass (COM) displacement of the convergent beam electron diffraction pattern, two offset vectors representing the sample's electric field are generated, and their integration yields the projected electrostatic potential of the sample expressed as an integrated DPC (iDPC) image[39]. Compared to high-angle annular dark field (HAADF)-STEM, iDPC-STEM utilizes independent advantages of low-dose imaging benefitting from the high-intensity low-angle scattered electrons;

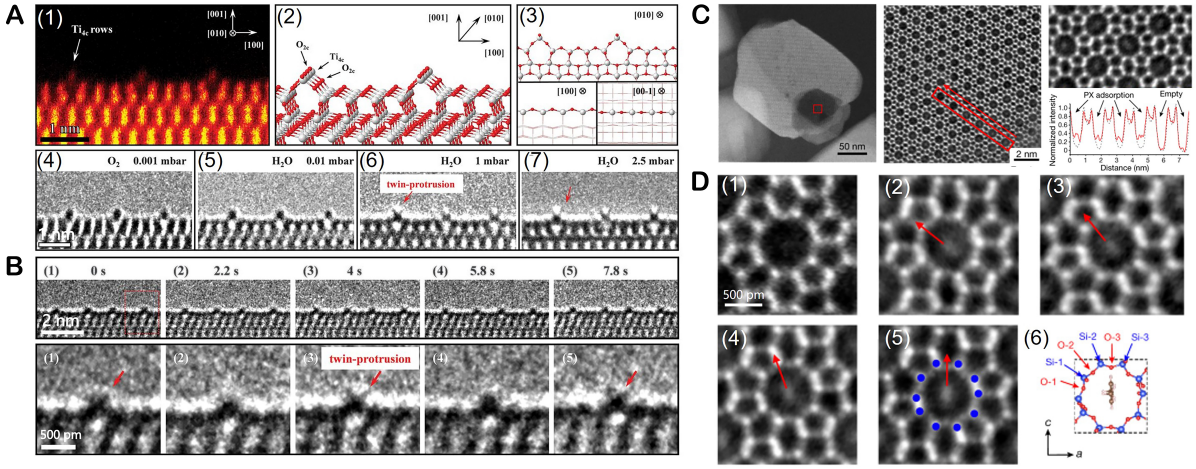

Figure 5. (A) Dynamic atomic structural evolution of the (1 × 4) reconstructed TiO_2(001) surface in a water vapor environment. Reprinted with permission from ref.[19] Copyright 2020 AAAS. (B) Sequential ETEM images show the dynamic structural evolution of the Ti row. (C) Imaging single para-xylene (PX) molecules in the straight channels of ZSM-5. (D) Identifying different orientations of PX pointer molecules. Reprinted with permission from ref.[47] Copyright 2021 Springer Nature.

meanwhile, it also naturally reduces the noise through vector numerical integration upon the differential signal, thereby maintaining commendable signal-to-noise ratios under low-dose conditions. Additionally, the contrast in iDPC images correlates nearly linearly with atomic numbers, facilitating simultaneous imaging of light and heavy elements, such as Li, Be, B, C, O, *etc.*, and aiding in the direct visualization of reactant and product molecules on the catalyst surface[40]. With the application of *in-situ* cameras featuring high quantum detection efficiency (DQE) and temporal resolution in TEM imaging, which reaches up to millisecond and single electron detection for a direct detector such as Gatan K3, the restructuring dynamics of working catalyst could be recorded, particularly in beam sensitive systems[41,42]. Accompanied with the low-dose imaging, algorithms for denoising the high resolution TEM/STEM images have also been developed to maximize the microstructure information and, accordingly, improve the temporal resolution further[43]. These comprehensive techniques unravel the high spatiotemporal details of metal particle restructuring, even anion vacancies, in a quantitative way when jointly utilizing artificial intelligence (AI)-assisted feature detection and data-mining methodologies[44]. Besides the above camera applications for information recording in parallel imaging mode, hybrid pixel detectors (HPD), which emphasize fast recording (up 10^2 KHz) at enhanced dynamic range (10 pA/pixel), are specially designed for the rising technique of four-dimensional (4D)-STEM and are attracting increasing attention. The diffraction patterns can be recorded at each scanning position of the electron beam on the sample in STEM mode. In the acquired 2D images, each pixel contains a complete 2D diffraction pattern, resulting in data with four dimensions, commonly referred to as 4D STEM. Specifically, 4D-STEM multislice ptychography has proven to be an efficient low-dose 3D imaging technique, capable of identifying individual framework oxygen (O) atoms in MFI (Mobil Five) zeolites and accurately determining the orientations of adsorbed molecules[45]. It also facilitates the dose-efficient diffraction imaging of the organic molecular thin films[46].

As illustrated in Figure 5C, Shen *et al.* employed alkaline reagents to etch ZSM-5 crystals, precisely controlling the sample thickness between 4 and 6 nm[47]. With the strategic selection of appropriate probe molecules and "freezing" guest molecules within zeolite nanopores, the ability of iDPC-STEM to image light elements under low-dose conditions was harnessed. Utilizing the penetrating straight channels of ZSM-5 as windows, atomic-resolution iDPC-STEM images of single reactant molecules were successfully obtained, enabling the identification of the orientation of para-xylene (PX) molecules and changes in channel

geometry [Figure 5D]. This approach realized the dynamic evolution process of gas molecules entering or leaving the zeolite framework and the geometric changes in the pore openings of corresponding channels, unveiling the intrinsic mechanisms governing molecule breakthroughs in pore size limitations. The operando TEM, grounded in iDPC-STEM and precise sample control, lays an efficient option for exploring dynamic processes such as gas molecule adsorption and desorption, diffusion, chemical bond formation and breakage, or lattice vibration. This methodology holds promising prospects for advancing our understanding of the structure-activity relationship[47-50].

Chip modification for catalytic reactions

The application of various external fields in electron microscopy is facilitated using MEMS-based devices in *in situ* electron microscopy. The MEMS chip functions as a carrier for directly holding the specimen and as a medium for introducing external fields, playing an indispensable role in testing catalyst performance. The integration of MEMS chips constitutes an effective approach for realizing operando TEM. Beyond applications of promoting kinetics of chemical reactions, catalytic metals find extensive use as gas sensors and related fields; Pt and Pd are employed to enhance the performance of gas sensors based on semiconductor metal oxides (SMO)[51,52]. However, these gas sensors (SMO) typically operate in ambient air at temperatures as high as several hundred degrees, leading to catalyst deactivation[53,54]. To comprehend the deactivation mechanism, studying the structural evolution of the catalyst in an H_2 sensor is imperative, establishing the structure-activity relationship under operational conditions[55]. Wang *et al.* fabricated an H_2 sensor by *in situ* growth of ZnO nanowire (NW) arrays on a MEMS chip and self-assembled Pd-Ag nanoparticles on the ZnO NWs[56]. They conducted H_2 sensing performance tests to establish an operando TEM setup. The comprehensive observation of the morphology and phase evolution of the Pd-Ag alloy nanoparticle catalyst under working conditions [Figure 6A] unveiled the deactivation mechanism of the alloy nanoparticle catalyst at various operating temperatures. Building on this understanding, the hydrogen sensor was optimized, effectively advancing the practical utility of hydrogen sensors[56].

TGA, a seminal catalytic analytical technique, finds extensive applications in evaluating catalyst performance and conducting component analysis[57-59]. In conventional thermogravimetric analyzers, a thermobalance with a mass resolution of sub-microgram is essential for tracking the catalytic mass loss during a temperature-programmed reaction. Typically, milligram-level specimens are consumed to acquire quantitative TGA curves, which contain temperature-related mass changes. These curves provide crucial insights into material structure, composition, thermal stability, and reaction kinetics. Based on MEMS technology, Li *et al.* integrated a mass-change resonant micro-cantilever and a controllable self-heating function on the ultra-thin SiN_x supporting film. This innovative approach enables the simultaneous analysis of microstructure evolution accompanied with reaction-induced thermogravimetry (TG), denoted as TG-TEM [Figure 6B][60]. This methodology provides particularly valuable insights for comprehending the structural evolution of catalysts during reactions. Additionally, using the micro-cantilever, characterization techniques such as H_2-TPR can also be implemented [Figure 6C][61]. The microreactor-based TG/TPR-TEM simultaneous analysis gives rise to an integrated characterization platform, expanding the avenues for realizing operando TEM.

TEM image-based microstructure quantification and activity correlation

Microscopic imaging offers real spatial information about materials, involving a high diversity of catalyst structural information, such as morphology, phase, atomic structure, surface crystal planes, and interface structure. This information is pivotal for determining the unfolding catalytic activity. However, the limitation of microscopic imaging in providing localized microstructural details makes it challenging to elucidate the overall structural status of catalysts that are actually in the same range yielding detectable activity, that is, the loss of spatial consistency between microstructure analysis and performance evaluation.

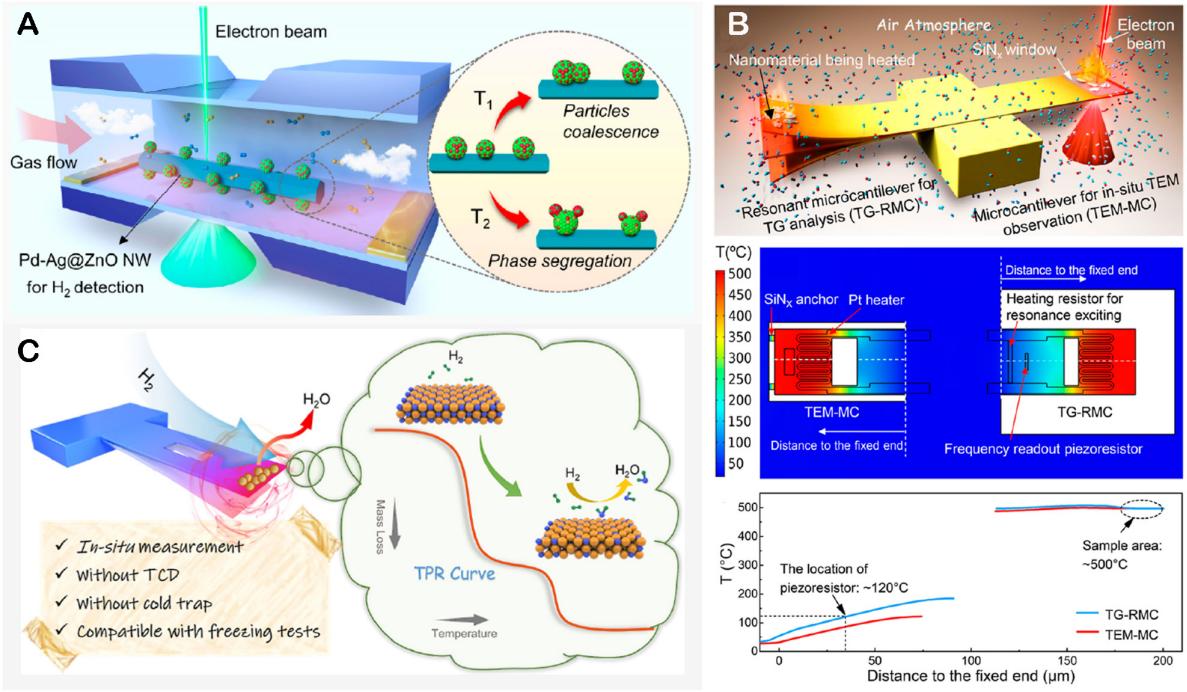

Figure 6. (A) The *in situ* TEM schematic view of the ZnO-based H_2 sensor with Pd-Ag alloy nanoparticles as the catalyst. Reprinted with permission from ref.[56] Copyright 2022, American Chemical Society. (B) The schematic view of the microcantilever-based TG-TEM microchip for operando TEM and the thermal simulation results for temperature distribution on both TG-RMC and TEM-MC during heating. Reprinted with permission from ref.[60] Copyright 2022, American Chemical Society. (C) The schematic view and working principle of the microcantilever-based *in situ* H_2-TPR. Reprinted with permission from ref.[61] Copyright 2022, American Chemical Society.

Taking supported metal catalysts as an example, the atomic dispersion characteristics (such as atomic density, inter-atom distances, and local coordinating environments) directly modulate the reaction activity, selectivity, and stability, thereby structurally influencing catalytic performance. Describing the atomic details through the minority of TEM images falls short of reflecting the comprehensive atomic dispersion status of the whole catalyst. In such instances, it becomes imperative to conduct ahigh-throughput analysis over TEM data large enough to establish macroscale structural statistics. This approach enables the correlation of microstructural details with macroscopic properties, facilitating the establishment of the structure-activity relationship of catalysts under working conditions. It is, therefore, included as an extended operando TEM methodology.

The tracking of material transformations and chemical reactions in *in situ* TEM generates substantial electron microscopy data in the form of images. Traditional manual processing and analysis of these voluminous datasets are laborious and time-consuming, with the potential for human bias-induced erroneous conclusions. Machine learning empowers computer systems to execute specific tasks based on data and experience, constructing computational models and algorithms[62]. Fueled by the proliferation of massive data, sophisticated computer algorithms, and advancements in computing hardware, notably the evolution of graphics processing units (GPUs), "deep learning" has emerged. As depicted in Figure 7A, deep learning executes intricate recognition processes by breaking down images into simple yet non-linear mathematical operations. It constructs neural networks for object recognition, associating input images with correct output labels[63,64].

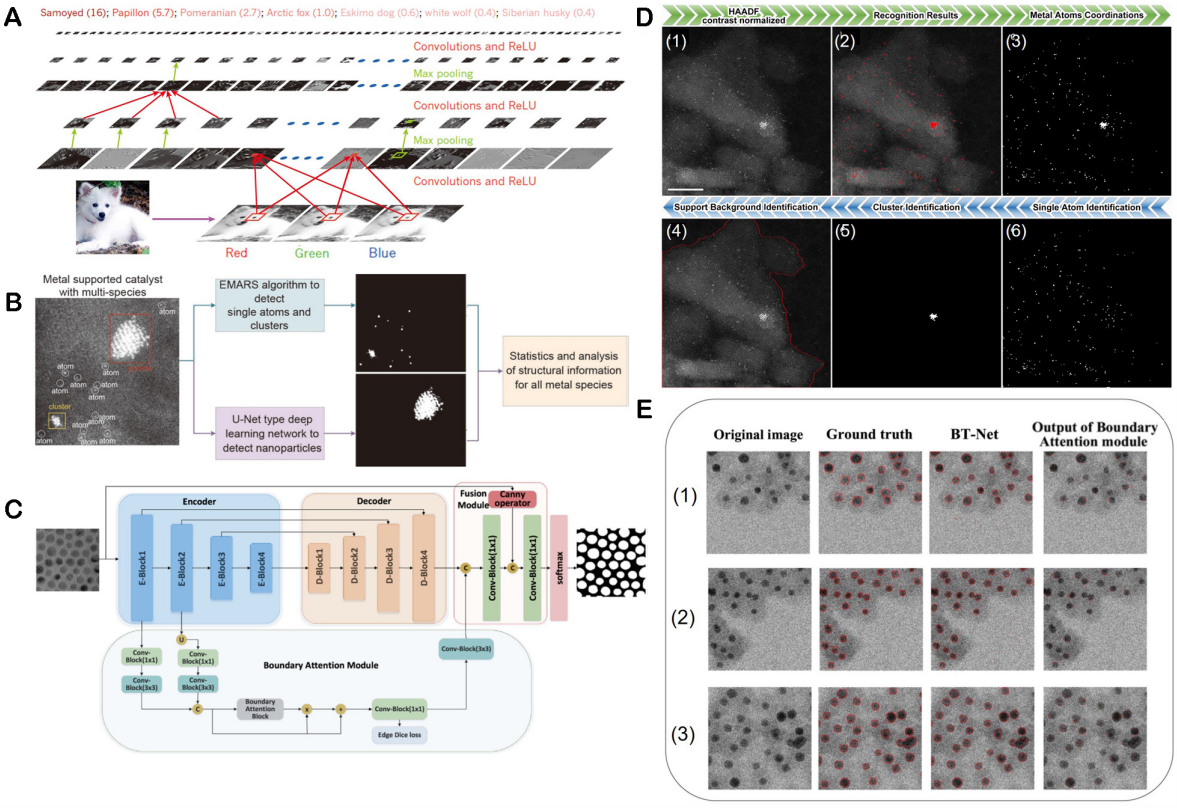

Figure 7. (A) The outputs of each layer of a typical convolutional network architecture applied to the image of a Samoyed dog; each rectangular image is a feature map corresponding to the output for one of the learned features, detected at each image position[64]. Copyright 2015 Springer Nature. (B) The schematic view of all-metal species quantification process. (C) Architecture of BT-Net, which includes the main encoder-decoder framework, the boundary attention module to extract the edge information of nanoparticles and the fusion module. (D) Visualized performance of electron-microscopy-based atom recognition statistics (EMARS) analysis procedures applied on a HAADF image of Pt/Al_2O_3 reforming catalyst[65].Copyright 2021, American Chemical Society. (E) Visualization of nanoparticle identification results with core-shell structure. (C and E) have been reproduced from ref.[66] Copyright 2021, Elsevier.

The development of atom-revolved macroscale structure evaluation has been realized, namely the electron-microscopy-based atom recognition statistics (EMARS, Figure 7B and C) method[65] and a deep learning-driven nanoparticle segmentation algorithm based on HAADF images [Figure 7D and E][66], which enable the identification and quantification of atomic coordinates, sizes, and profiles for all metal species in the system and the profile of the catalyst carrier, achieving comprehensive quantification of metal species. Leveraging high-throughput atomic-resolution electron microscopy data, a statistical analysis of atomic-level dispersion in real space was conducted. This approach surpasses the limitations of traditional electron microscopy focused on micro-region characterization. It establishes a connection from microstructural details to macroscopic performance, allowing for the correlation of the microstructure to determine the genuine active sites of the catalyst and fostering a deeper understanding of the actual catalytic process.

OPERANDO TEM PRACTICAL APPLICATION

To date, the operando TEM has emerged as a valuable tool providing crucial insights into the structural and morphological evolution of catalysts in their working state. This is achieved by integrating online mass spectrometry or EELS technology to track catalytic transformations within the TEM, finding applications in numerous gas-solid phase catalytic reactions. A prototypical example is the study of the CO oxidation reaction, a well-known heterogeneous reaction considered elementary. Investigation into the interaction of

simple molecules with precisely defined materials, such as CO oxidation, aids in comprehending chemical reactions and offers effective avenues for gaining insights into the chemical intricacies of coupled gas-surface reactions with heightened precision.

Vendelbo *et al.* pioneered operando TEM by integrating the gas cell system with quantitative analysis of mass spectrometry and reaction calorimeter[67]. This groundbreaking approach allowed simultaneous high-resolution TEM observation, product gas composition analysis, and calorimetric detection throughout the reaction process. The periodic structural oscillations of Pt nanoparticles were observed during the CO oxidation reaction. *In situ* mass spectrometry revealed that these oscillations were synchronized with O_2 and CO partial pressure oscillations, contrary to CO_2 partial pressure oscillations. Simultaneously, these oscillations matched the thermal release/absorption, as depicted in Figure 8A. The study concluded that the CO oxidation reaction activity correlates with the dynamically evolving exposed crystal facets of Pt nanoparticles. This provided direct evidence and insights into the interplay between catalytic reactions and the dynamic shape dynamics of catalyst nanoparticles[67]. Similarly, Ghosh *et al.* uncovered a similar phenomenon during the CO oxidation reaction catalyzed by Pd nanoparticles through operando TEM[68]. They investigated the oscillations of Pd nano-octahedra and truncated nanocubes during the CO oxidation reaction, finding that the corners of nano-octahedra were flat at the low-activity state and rounded at the high-activity state, with these corners periodically reconstructed and oscillated with the reaction rate [Figure 8B(1)-(3)]. Compared to the non-oscillating nanocubes, the oscillations of truncated nanocubes indicate the crucial importance of (111) crystal facets for the oscillatory behavior, as shown in Figure 8B(4)-(7). Combined with theoretical calculations, it is shown that the oscillatory behavior is related to differences in CO adsorption coverage and subsequent changes in surface energies of different facets. These two operando TEM studies collectively demonstrate that the real-time changing structure of the catalyst continuously modulates catalytic activity. Moreover, they extend the relevance of this dynamic structural activation-deactivation behavior of nanoparticles to various other catalyst systems, thereby expanding our understanding of CO oxidation on metal nanoparticles. This understanding is pivotal for guiding the design of future high-performance catalysts[68].

Miller *et al.* accomplished a high catalyst loading by concurrently employing RGA and EELS (Section "Direct detection of catalytic products") to assess product gas composition and conversion rates within the ETEM setup[69]. Through this setup, they quantified chemical reaction kinetics and calculated reaction rates and rate constants, all while conducting atomic resolution imaging via operando TEM. The study revealed that under CO oxidation reaction conditions, the Ru nanoparticle catalyst developed thin RuO_2 layers (~0.5 nm) [Figure 8C(1)-(2)]. However, by correlating the structural evolution with the reaction rate, it was discerned that the activity of these oxide layers is considerably lower than that of the exposed Ru particle surface. Eliminating these RuO_2 layers resulted in heightened catalyst activity [Figure 8C(3)]. This substantiates that the thin RuO_2 layer formed merely covers the surface of Ru nanoparticles as a bystander species, challenging the conventional belief that it serves as an active species[69]. Moreover, Yuan *et al.* demonstrated the adsorption of water molecules on the Ti_{4c} site on the surface of anatase TiO_2 in a double protrusion structure[19]. This site was identified as an active site for both H_2O adsorption dissociation and the water-gas shift reaction. The direct visualization of adsorption and desorption sites and reaction processes of reactants and product molecules on the catalyst surface provides persuading evidence of catalyst active sites. By judiciously selecting catalyst materials and reactant molecules, reaction active sites can be determined under working conditions.

Chen *et al.* utilized the single-molecule imaging technology outlined in Section "Direct observation of reactant or product molecules" to observe the movement and evolution of single molecules within the

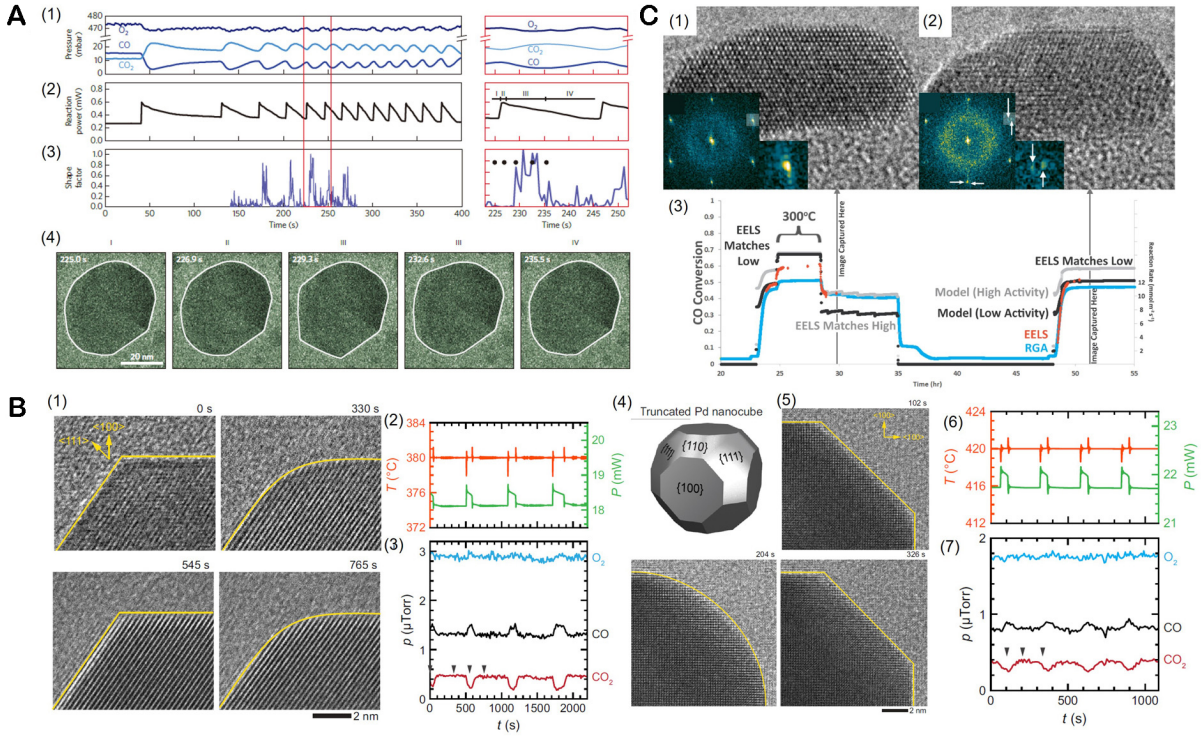

Figure 8. (A) Correlation of oscillatory CO oxidation reaction data with the projected morphology of a Pt nanoparticle. (1-3) Mass spectrometry of the CO, O_2 and CO_2 pressures, reaction power and shape factor for the Pt nanoparticle in (4) as a function of time. (4) Time-resolved TEM images of a Pt nanoparticle at the gas exit of the reaction zone[67]. Copyright 2014 Springer Nature. (B) Restructuring of Pd nano-octahedron (1) and truncated nanocube (5) during an oscillatory CO oxidation reaction. And the plots of the measured temperature, heater power, and the corresponding amounts of the CO, O_2, and CO_2 gases during CO oxidation reaction of Pd nano-octahedron (2) and (3) and truncated nanocube (6) and (7). (4) The schematic of a truncated nanocube[68]. Copyright 2022, Springer Nature. (C) The images of the same Ru particle in the high (1) and low activity (2) states. (3) CO conversion obtained using both EELS and RGA is plotted for the operando experiment along with two calculated CO conversion curves based on an Arrhenius fit to plug flow reactor data[69]. Copyright 2021, American Chemical Society.

ZSM-5 zeolite channels at the atomic scale[49]. Figure 9A depicts the schematic of the *in situ* STEM experimental setup during benzene adsorption and desorption. As illustrated in Figure 9B, upon the adsorption of benzene molecules, the straight channels in the initially perceived rigid zeolite frameworks underwent pronounced local deformation along the unified direction of the benzene molecules, allowing for the diffusion of larger molecules. The geometry of the zeolite pore deformation and the arrangement and direction of the restricted benzene molecules mutually constrained each other, maintaining the overall MFI zeolite single crystal structure almost unchanged. This subcellular topological flexibility primarily emanates from the soft Si-O-Si hinge between the rigid tetrahedral SiO_4. These findings validate the capability of Electron Microscopy in directly imaging and analyzing small molecules, laying a robust foundation for the real-time analysis of dynamic reaction processes, such as molecular adsorption, desorption, and diffusion. It is anticipated that the complete real-time analysis of the dynamic reaction behavior of single molecules under working conditions can be achieved to track and observe the transformation process from reactant molecules to product molecules[49].

The calcination process holds a pivotal role in preparing and controlling functional materials. However, the conventional approach to calcination relies on accumulated laboratory research experience, lacking the necessary support from theoretical or experimental data. Zhou *et al.* conducted a meticulous observation of the morphological evolution of the precursor under atmospheric conditions using *in situ* TEM[70]. They

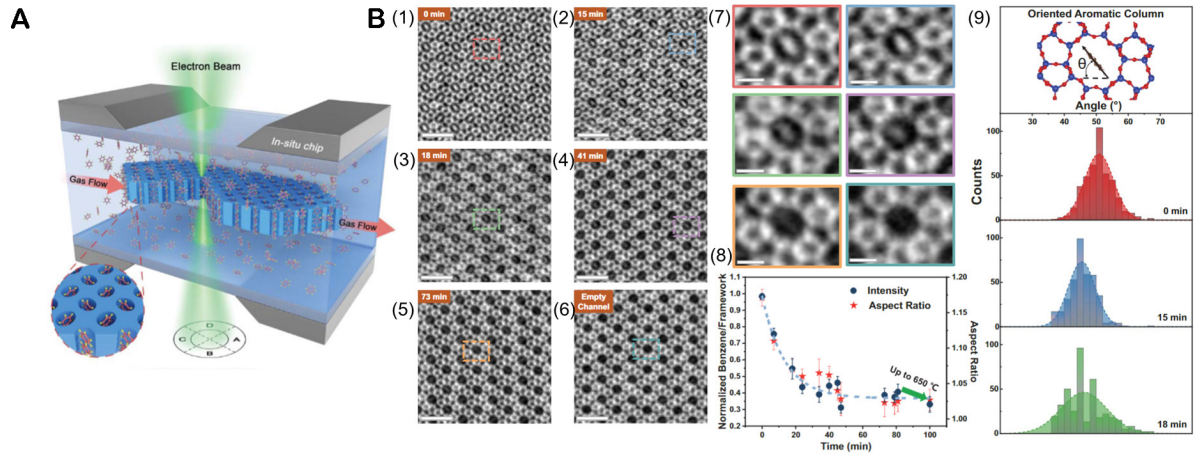

Figure 9. (A) The schematic of the *in situ* STEM experimental setup during benzene adsorption and desorption. (B) Dynamic evolution of zeolite channels and corresponding host-guest interactions in benzene desorption. (1)-(6) iDPC-STEM snapshots of a benzene@MFI specimen along the [010] projection at different stages during the cyclic benzene desorption process. (7) Magnified iDPC-STEM images of straight channels extracted from (1) to (6), indicating the changes in benzene contrast and channel geometry at different stages. (8) Evolution of the normalized benzene/zeolite framework contrast ratio and corresponding aspect ratios of Si_{10} opening pores during the *in situ* benzene uptake and release process. (9) Statistical distribution of benzene orientations at different stages of benzene desorption. Scale bars, 2 nm [(1) to (6)], 500 pm (7)[49]. Copyright 2022, AAAS.

determined the correct calcination temperature through cantilever-based TGA [Figure 10A]. In an environment containing H_2, it was discovered that the MnO_2 precursor could be converted into Mn_3O_4 with favorable electrical properties at a remarkably low calcination temperature of 400 °C. Notably, the structure of the MnO_2 precursor NW was well-preserved during this phase transformation [Figure 10B][70]. This collaborative characterization method, integrating microreactor-based spectroscopy and TEM, exhibits significant application potential in material preparation, thereby expanding the avenues for investigating operando TEM.

In recent progress, the integration of deep learning into microscopic imaging analysis has primarily centered on extracting quantitative information via high throughput analyzing microscopy data to elucidate macroscale statistics upon a catalyst sample in aspects of its morphology, coordinates, defects, metal dispersion, and even dynamic structures tracking. As one pioneered work of analyzing metal atom dispersion in a practical industry catalyst, Liu *et al.* conducted a statistical analysis of over 18,000 Pt atoms on the Pt/Al_2O_3 reforming catalyst, yielding the Pt-Pt atomic distance distribution within the range of 23 picometers to 60 angstroms and determining the number of atoms contained in all Pt clusters[65]. This application of the EMARS algorithm redefined the metal dispersion of the supported catalyst with atomic precision in real space [Figure 11A]. The statistical findings revealed that the aromatic conversion activity in naphtha reforming arises from Pt single atoms on the support, with the density of single-atom Pt quantitatively linked to the reforming activity. Pt clusters, while not directly contributing to activity, can dynamically disperse into Pt single atoms under an oxidizing atmosphere to supplement active sites [Figure 11B].

Moreover, by combining EMARS with particle segmentation using the U-net network, a full metal species quantification (FMSQ) upon complex multi-species containing supported catalyst could be metal[71]. This method facilitated the quantitative depiction of the gold dispersion of all microstructured species, ranging from single atoms to clusters and irregular-shaped particles supported on NC and C_3N_4 [Figure 11C]. By correlating the fractions of Au species in a series of samples with their catalytic activities of butadiene

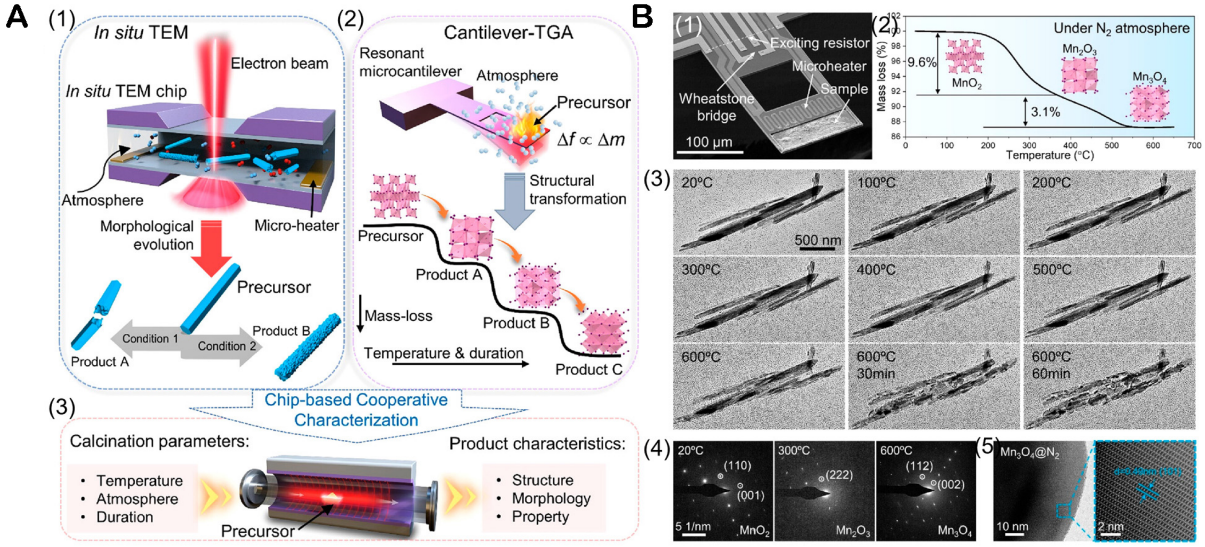

Figure 10. (A) Concept of the cooperative characterization approach. (1) *In situ* TEM observes the morphological evolution of the material under different calcination conditions. (2) Cantilever-TGA gives the detailed calcination temperature and duration. (3) Cooperative characterization with *in situ* TEM and cantilever-TGA provides a comprehensive calcination parameter and can tune the product characteristics. (B) Calcination results of MnO_2 nanowires under an N_2 atmosphere. (1) SEM image of the resonant microcantilever for the cantilever-TGA measurements. (2) Cantilever-TGA curve of the MnO_2 nanowires under an N_2 atmosphere. Two mass-loss stages can be distinguished and correspond to the production of Mn_2O_3 and Mn_3O_4, respectively. (3) *In situ* TEM results of the MnO_2 nanowires under an N_2 atmosphere. (4) SAED patterns of the sample obtained at different temperatures. (5) Cs-corrected TEM images of the sample obtained at 600 °C for 1 h[70]. Copyright 2023, American Chemical Society.

hydrogenation (BDH) [Figure 11D], it indicated that activity of single atoms is low, and BDH activity was actually associated with the formation of gold nanoparticles. This objective and accurate microscopic atomic dispersion analysis of catalysts based on deep learning and *in situ* electron microscopy establishes a direct correlation between macroscale performance and atomic-scale microstructure.

SUMMARY AND PERSPECTIVE

The advancements of *in situ* TEM technology have opened unprecedented avenues for unraveling the functionality principles in fields of energy materials and catalytic chemistry. By replicating actual reaction conditions within the TEM, it becomes feasible to track the dynamics of atomic structures and composition constitutions. Further realization of operando TEM offers distinct advantages in establishing catalytic structure-activity relationships, particularly pinpointing the genuine active sites. This aligns with the increasing demand of discovering new catalytic mechanisms to fabricate new catalysts for promoted reaction performances.

Focusing on the recent progress of operando TEM technology, this review broadens its definition by demonstrating more newly emerged approaches of measuring a catalytic reaction inside a transmission electron microscope (TEM), including gas reaction, direct observation of gas molecules, electron microscopy-multiple spectroscopies, and TEM image-based microstructure quantification and activity correlation. Various applications and discovered results using these advanced techniques have been introduced, underscoring the potential of operando TEM in gas-phase catalytic reactions.

While operando TEM has showcased remarkable potential and progress, it also confronts limitations and challenges, leaving ample room for improvement in related instruments and research methodologies. One

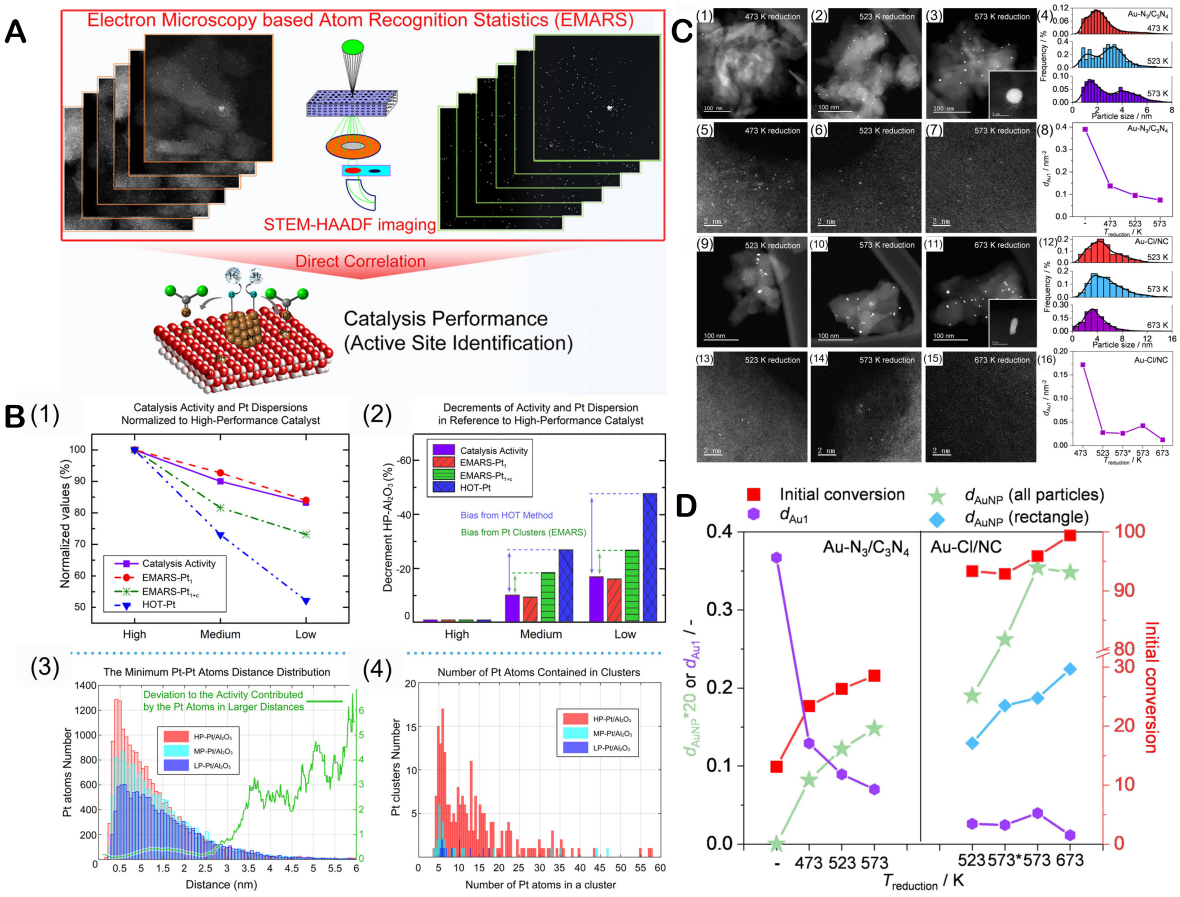

Figure 11. (A) Demonstration on advantages of EMARS for the dispersion analysis of metal-supported catalyst. (B) Correlation between Pt species dispersion and catalytic activity of aromatics production quantitatively analyzed via EMARS and HOT methods. (1) Normalized catalysis activity and Pt species dispersions. (2) Bias of dispersion calculation in reference to the activity. (3) Overall distribution of Pt-Pt atom distances for catalysts of high, middle, and low performances, respectively; a profile (green) is also derived about the deviation to the activity from the integrated contribution of Pt atoms along with larger distances. (4) Histogram of atom numbers contained in Pt clusters[65]. Copyright 2021, American Chemical Society. (C) Full metal species quantification of Au components through automated electron microscopic analyses of reduced catalysts. HAADF-STEM images of Au-N_3/C_3N_4 (1)-(3) and (5)-(7) and Au-Cl/NC (9)-(11) and (13)-(15). The insets in (3) and (11) show the enlarged images of the respective Au particles with distinct shapes. (4) and (12) The Au particle size distributions obtained through particle unit recognition, and (8) and (16) the densities of single atoms as a function of the reduction temperatures analyzed by EMARS. (D) Correlations of FMSQ results of the Au catalysts with the hydrogenation activity[71]. Copyright 2022, Wiley.

primary challenge involves the transformation of MEMS-based nanochips for operando TEM. To gauge the catalytic conversion activity of a catalyst in TEM accurately, it is necessary to enlarge the reaction area of the supporting MEMS chip to load a sufficient quantity of catalyst specimens to generate a discernible product signal. However, increasing the heating area would inevitably induce the silicon frame to bulge out of imaging focus during *in situ* observation. Commercial chips often mitigate this heating instability by minimizing the heating area to reduce drift and promote temperature uniformity[72]. One efficient way to overcome the above trade-off relationship is to *in situ* measurement of specimen drift and automatic correction[73]. By adopting this approach, the heating area on chips can be expanded to carry enough catalyst to satisfy the requisites of operando TEM. Simultaneously, incorporating a 2nd microheater in the non-observation area of the MEMS chip beside the existing imaging zone turns to another strategy for ensuring product detection without compromising the imaging resolution. Additionally, integrating a chemical sensor into the MEMS chips would enable target-specified reaction detection, providing an alternative approach to measure the catalytic activity while probing the microstructures.

Moreover, it is worth noting that a significant discrepancy exists between fixed-bed and gas-cell reactors in TEM, impeding the further advancement of operando TEM. It encompasses variations in gas flow rate, contact modes between reactants and catalysts, and synergistic effects among catalyst particles due to the differences of heat transfer and particle stacking. Evaluating the dynamics between these two systems proves challenging due to inherent difficulties in comparing models with real systems. Additionally, the typical reaction pressure in practical catalytic reactions could reach up to MPa level, surpassing the maximum pressure in the gas cell system, not to mention the conditions in ETEM. Gas cell technology, designed for thinner windows, higher pressures, and compatibility with multi-environment coupling, is demanded and continually evolving. Enhancements may involve fortifying the mechanical strength and chemical resistance of liquid or gas cell window films to further reduce film thickness, improving imaging quality, or achieving higher reaction pressure. Integrating gas cell technology with ETEM can be achieved by adding micro-holes to the upper chip in the nanoreactor[74], facilitating electron beam passage to enhance image resolution and accommodate higher gas pressure in ETEM. By refining the ventilation method in ETEM and augmenting gas flow rates near the specimen, the reaction efficiency under low pressure can closely mimic real reactions. Besides, the influence of beam irradiation shall always be kept in mind when performing the experiments. An irradiation influence could not be completely avoided since mass-electron interaction permanently exists but could be minimized by pre-setting beam energy below a critical threshold in samples dominated by knock-on damage, e.g., 2D materials, or reducing the dose rate to satisfy relatively imaging over samples sensitive to radiolysis damages, such as zeolites and organic frameworks[75]. Practically, a benchmark experiment helps determine such threshold of beam energy or dose rate. Other alternatives for evaluating beam irradiation influence include turning off the electron beam when running the *in situ* reaction and afterward checking the structure difference between this blanked sample and its continuously irradiated counterparts. One should also be conscious of the beam-activated reaction atmosphere upon inducing reconstruction bias of the catalyst; for example, a CO_2 molecule could easily oxidize the 3d-metals under room temperature in beam irradiation.

Finally, TEM imaging is traditionally perceived as a highly localized micro-area technology providing localized structural and chemical information about the catalyst, but the relevant length and time scales of catalytic processes often span several orders of magnitude. Hence, developing collaborative *in situ* methods combining TEM with other technologies (X-ray, Raman, *etc.*) emerges as a future trend. Through real-space *in situ* observation combined with various spectroscopy methods, it enriches the understanding of microstructure evolution across different scales. Presently, it is challenging to modify a commercial ETEM system for providing various external fields (light, plasma, microwave, *etc.*) due to the limited objective chamber geometry. In this context, it is urgent to develop integrated multi-field coupling devices using the MEMS chip technique to further advance operando TEM methodology. New opportunities could be expected thanks to the rising attention of energy catalysis research boosted by the world background of carbon peaking and carbon neutrality.

DECLARATIONS

Authors' contributions

Summarized and wrote original draft: Zhang F

Made substantial contributions to conception and design of the review: Liu W

Availability of data and materials

Not applicable.

Financial support and sponsorship

This work is supported by the National Natural Science Foundation of China (22072150), Outstanding Member of the CAS Youth Innovation Promotion Association, and CAS Project for Young Scientists in Basic Research (YSBR-022).

Conflicts of interest

All authors declared that there are no conflicts of interest.

Ethical approval and consent to participate

Not applicable.

Consent for publication

Not applicable.

REFERENCES

1. Chorkendorff I, Niemantsverdriet JW. Concepts of modern catalysis and kinetics. Weinheim: Wiley-VCH; 2003. DOI
2. deJong KP. Synthesis of solid catalysts. Weinheim: Wiley-VCH; 2009. DOI
3. Liu L, Corma A. Evolution of isolated atoms and clusters in catalysis. *Trends Chem* 2020;2:383-400. DOI
4. Cao S, Tao FF, Tang Y, Li Y, Yu J. Size- and shape-dependent catalytic performances of oxidation and reduction reactions on nanocatalysts. *Chem Soc Rev* 2016;45:4747-65. DOI
5. Calle-Vallejo F, Loffreda D, Koper MT, Sautet P. Introducing structural sensitivity into adsorption-energy scaling relations by means of coordination numbers. *Nat Chem* 2015;7:403-10. DOI PubMed
6. Groppo E, Rojas-Buzo S, Bordiga S. The role of in situ/operando IR spectroscopy in unraveling adsorbate-induced structural changes in heterogeneous catalysis. *Chem Rev* 2023;123:12135-69. DOI PubMed PMC
7. Sun Y, Deng Y, Chen H, Yang X, Lin X, Li J. Design strategies and in situ infrared, Raman, and X-ray absorption spectroscopy techniques insight into the electrocatalysts of hydrogen energy system. *Small Struct* 2023;4:2200201. DOI
8. Sarma BB, Maurer F, Doronkin DE, Grunwaldt JD. Design of single-atom catalysts and tracking their fate using operando and advanced X-ray spectroscopic tools. *Chem Rev* 2023;123:379-444. DOI PubMed PMC
9. Green IX, Tang W, Neurock M, Yates JT Jr. Spectroscopic observation of dual catalytic sites during oxidation of CO on a Au/TiO_2 catalyst. *Science* 2011;333:736-9. DOI PubMed
10. Yang J, Liu W, Xu M, et al. Dynamic behavior of single-atom catalysts in electrocatalysis: identification of Cu-N_3 as an active site for the oxygen reduction reaction. *J Am Chem Soc* 2021;143:14530-9. DOI
11. Zhang S, Nguyen L, Zhu Y, Zhan S, Tsung CK, Tao FF. In-situ studies of nanocatalysis. *Acc Chem Res* 2013;46:1731-9. DOI PubMed
12. Dessal C, Len T, Morfin F, et al. Dynamics of single Pt atoms on alumina during CO oxidation monitored by *operando* X-ray and infrared spectroscopies. *ACS Catal* 2019;9:5752-9. DOI
13. Su DS, Zhang B, Schlögl R. Electron microscopy of solid catalysts - transforming from a challenge to a toolbox. *Chem Rev* 2015;115:2818-82. DOI PubMed
14. Tao FF, Crozier PA. Atomic-scale observations of catalyst structures under reaction conditions and during catalysis. *Chem Rev* 2016;116:3487-539. DOI PubMed
15. Boyes ED, LaGrow AP, Ward MR, Martin TE, Gai PL. Visualizing single atom dynamics in heterogeneous catalysis using analytical in situ environmental scanning transmission electron microscopy. *Philos Trans A Math Phys Eng Sci* 2020;378:20190605. DOI PubMed PMC
16. Maurer F, Jelic J, Wang J, et al. Tracking the formation, fate and consequence for catalytic activity of Pt single sites on CeO_2. *Nat Catal* 2020;3:824-33. DOI
17. Muravev V, Spezzati G, Su Y, et al. Interface dynamics of Pd-CeO_2 single-atom catalysts during CO oxidation. *Nat Catal* 2021;4:469-78. DOI
18. Frey H, Beck A, Huang X, van Bokhoven JA, Willinger MG. Dynamic interplay between metal nanoparticles and oxide support under redox conditions. *Science* 2022;376:982-7. DOI PubMed
19. Yuan W, Zhu B, Li XY, et al. Visualizing H_2O molecules reacting at TiO_2 active sites with transmission electron microscopy. *Science* 2020;367:428-30. DOI
20. Zhang X, Han S, Zhu B, et al. Reversible loss of core-shell structure for Ni-Au bimetallic nanoparticles during CO_2 hydrogenation. *Nat*

Catal 2020;3:411-7. DOI
21. Crozier PA, Hansen TW. *In situ* and *operando* transmission electron microscopy of catalytic materials. *MRS Bull* 2015;40:38-45. DOI
22. Chee SW, Lunkenbein T, Schlögl R, Cuenya BR. In situandoperandoelectron microscopy in heterogeneous catalysis-insights into multi-scale chemical dynamics. *J Phys Condens Matter* 2021;33:153001. DOI PubMed
23. Bañares MA, Wachs IE. Molecular structures of supported metal oxide catalysts under different environments. *J Raman Spectrosc* 2002;33:359-80. DOI
24. Marton L. Electron microscopy of biological objects. *Nature* 1934;133:911. DOI
25. Creemer JF, Helveg S, Hoveling GH, et al. Atomic-scale electron microscopy at ambient pressure. *Ultramicroscopy* 2008;108:993-8. DOI
26. Boyes E, Gai P. Environmental high resolution electron microscopy and applications to chemical science. *Ultramicroscopy* 1997;67:219-32. DOI
27. DENSsolutions. Climate: in situ TEM gas & heating. Available from: https://denssolutions.com/products/climate [Last accessed on 11 Jun 2024].
28. Perez-Garza HH, Morsink D, Xu J, Sholkina M, Pivak Y, et al. The "Climate" system: nano-reactor for in-situ analysis of solid-gas interactions inside the TEM. Proceedingsof the IEEE 11th Annual International Conference on Nano/Micro Engineered and Molecular Systems; 2016 April 17-20; Sendai, Japan. New York City: IEEE; 2016. pp. 85-90. DOI
29. Plodinec M, Nerl HC, Farra R, et al. Versatile homebuilt gas feed and analysis system for operando TEM of catalysts at work. *Microsc Microanal* 2020;26:220-8. DOI
30. Zhou D, Spruit RG, Pen M, Garza HP, Xu Q. Correlative in-situ gas and heating TEM: integrating calorimetry and mass spectroscopy. *Microsc Microanal* 2020;26:3044-6. DOI
31. Gross JH. Mass spectrometry: a textbook. Berlin: Springer International Publishing; 2017. DOI
32. DENSsolutions info. Discover how in situ TEM advances catalysis research. Available from: https://www.youtube.com/watch?v=A1LkGWZT4Ow [Last accessed on 11 Jun 2024].
33. Zhang F, Pen M, Spruit RG, Garza HP, Liu W, Zhou D. Data synchronization in operando gas and heating TEM. *Ultramicroscopy* 2022;238:113549. DOI PubMed
34. Chenna S, Crozier PA. Operando transmission electron microscopy: a technique for detection of catalysis using electron energy-loss spectroscopy in the transmission electron microscope. *ACS Catal* 2012;2:2395-402. DOI
35. Crozier PA, Chenna S. In situ analysis of gas composition by electron energy-loss spectroscopy for environmental transmission electron microscopy. *Ultramicroscopy* 2011;111:177-85. DOI PubMed
36. Miller BK, Barker TM, Crozier PA. Novel sample preparation for operando TEM of catalysts. *Ultramicroscopy* 2015;156:18-22. DOI PubMed
37. Miller BK, Crozier PA. Analysis of catalytic gas products using electron energy-loss spectroscopy and residual gas analysis for operando transmission electron microscopy. *Microsc Microanal* 2014;20:815-24. DOI PubMed
38. Yuan W, Wu H, Li H, et al. In Situ STEM determination of the atomic structure and reconstruction mechanism of the TiO_2 (001) (1 × 4) surface. *Chem Mater* 2017;29:3189-94. DOI
39. Lazić I, Bosch EGT, Lazar S. Phase contrast STEM for thin samples: integrated differential phase contrast. *Ultramicroscopy* 2016;160:265-80. DOI PubMed
40. Lazic I, Bosch EGT, Lazar S. Integrated differential phase contrast (iDPC) STEM. *Acta Crystallogr A Found Adv* 2017;73:C117-8. DOI
41. Zhu Y, Ciston J, Zheng B, et al. Unravelling surface and interfacial structures of a metal-organic framework by transmission electron microscopy. *Nat Mater* 2017;16:532-6. DOI
42. Meledina M, Watson G, Meledin A, Van Der Voort P, Mayer J, Leus K. Ru catalyst encapsulated into the pores of MIL-101 MOF: direct visualization by TEM. *Materials* 2021;14:4531. DOI PubMed PMC
43. Thomas AM, Crozier PA, Xu Y, Matteson DS. Feature detection and hypothesis testing for extremely noisy nanoparticle images using topological data analysis. *Technometrics* 2023;65:590-603. DOI
44. Li S, Lin J, Chen Y, et al. Growth anisotropy and morphology evolution of line defects in monolayer MoS_2: atomic-level observation, large-scale statistics, and mechanism understanding. *Small* 2024;20:e2303511. DOI
45. Zhang H, Li G, Zhang J, et al. Three-dimensional inhomogeneity of zeolite structure and composition revealed by electron ptychography. *Science* 2023;380:633-8. DOI
46. Wu M, Stroppa DG, Pelz P, Spiecker E. Using a fast hybrid pixel detector for dose-efficient diffraction imaging beam-sensitive organic molecular thin films. *J Phys Mater* 2023;6:045008. DOI
47. Shen B, Chen X, Wang H, et al. A single-molecule van der Waals compass. *Nature* 2021;592:541-4. DOI
48. Shen B, Wang H, Xiong H, et al. Atomic imaging of zeolite-confined single molecules by electron microscopy. *Nature* 2022;607:703-7. DOI
49. Xiong H, Liu Z, Chen X, et al. In situ imaging of the sorption-induced subcell topological flexibility of a rigid zeolite framework. *Science* 2022;376:491-6. DOI
50. Xiong H, Wang H, Chen X, Wei F. Atomic imaging of zeolites and confined single molecules by iDPC-STEM. *ACS Catal* 2023;13:12213-26. DOI
51. Abe H, Kimura Y, Ma T, Tadaki D, Hirano-iwata A, Niwano M. Response characteristics of a highly sensitive gas sensor using a

titanium oxide nanotube film decorated with platinum nanoparticles. *Sensor Actuat B Chem* 2020;321:128525. DOI

52. Kim J, Mirzaei A, Kim HW, Kim SS. Improving the hydrogen sensing properties of SnO_2 nanowire-based conductometric sensors by Pd-decoration. *Sensor Actuat B Chem* 2019;285:358-67. DOI
53. Meng J, Li H, Zhao L, et al. Triboelectric nanogenerator enhanced schottky nanowire sensor for highly sensitive ethanol detection. *Nano Lett* 2020;20:4968-74. DOI
54. Wang X, Xu P, Tang L, Chen Y, Li X. Nano beta zeolites catalytic-cracking effect on hydrochlorofluorocarbon molecule for specific detection of Freon. *J Mater Chem A* 2021;9:15321-8. DOI
55. Zhou T, Zhang T. Recent progress of nanostructured sensing materials from 0D to 3D: overview of structure-property-application relationship for gas sensors. *Small Methods* 2021;5:e2100515. DOI PubMed
56. Wang X, Li M, Xu P, Chen Y, Yu H, Li X. In situ TEM technique revealing the deactivation mechanism of bimetallic Pd-Ag nanoparticles in hydrogen sensors. *Nano Lett* 2022;22:3157-64. DOI
57. Abel BA, Snyder RL, Coates GW. Chemically recyclable thermoplastics from reversible-deactivation polymerization of cyclic acetals. *Science* 2021;373:783-9. DOI PubMed
58. Chi X, Li M, Di J, et al. A highly stable and flexible zeolite electrolyte solid-state Li-air battery. *Nature* 2021;592:551-7. DOI
59. Zou Z, Habraken WJEM, Matveeva G, et al. A hydrated crystalline calcium carbonate phase: calcium carbonate hemihydrate. *Science* 2019;363:396-400. DOI
60. Yao F, Xu P, Li M, et al. Microreactor-based TG-TEM synchronous analysis. *Anal Chem* 2022;94:9009-17. DOI
61. Li X, Xu P, Zhou Y, et al. In situ hydrogen temperature-programmed reduction technology based on the integrated microcantilever for metal oxide catalyst analysis. *Anal Chem* 2022;94:16502-9. DOI
62. Alpaydin E. Introduction to machine learning. MIT Press, 2020. Available from: https://mitpress.mit.edu/9780262012119/introduction-to-machine-learning [Last accessed on 11 Jun 2024].
63. Deng L, Yu D. Deep learning: methods and applications. *FNT Sign Process* 2014;7:197-387. DOI
64. LeCun Y, Bengio Y, Hinton G. Deep learning. *Nature* 2015;521:436-44. DOI PubMed
65. Liu S, Xu H, Liu D, et al. Identify the activity origin of Pt single-atom catalyst via atom-by-atom counting. *J Am Chem Soc* 2021;143:15243-9. DOI
66. Liu S, Xu C, Zhang Z, Zhao Q, Yao L, Liu W. Precisely identify the geometry of catalyst particles from S/TEM images via a boundary attention deep learning network. *Mater Today Commun* 2021;28:102728. DOI
67. Vendelbo SB, Elkjær CF, Falsig H, et al. Visualization of oscillatory behaviour of Pt nanoparticles catalysing CO oxidation. *Nat Mater* 2014;13:884-90. DOI
68. Ghosh T, Arce-Ramos JM, Li WQ, et al. Periodic structural changes in Pd nanoparticles during oscillatory CO oxidation reaction. *Nat Commun* 2022;13:6176. DOI PubMed PMC
69. Miller BK, Crozier PA. Linking changes in reaction kinetics and atomic-level surface structures on a supported Ru catalyst for CO oxidation. *ACS Catal* 2021;11:1456-63. DOI
70. Zhou Y, Li M, Zhang T, et al. Cooperative characterization of in situ TEM and cantilever-TGA to optimize calcination conditions of MnO_2 nanowire precursors. *Nano Lett* 2023;23:2412-20. DOI
71. Wang Y, Zhang F, Wang M, et al. Discerning the contributions of gold species in butadiene hydrogenation: from single atoms to nanoparticles. *Angew Chem Int Ed* 2022;61:e202214166. DOI
72. Omme JT, Zakhozheva M, Spruit RG, Sholkina M, Pérez Garza HH. Advanced microheater for in situ transmission electron microscopy; enabling unexplored analytical studies and extreme spatial stability. *Ultramicroscopy* 2018;192:14-20. DOI PubMed
73. Zhang F, Zhang X, Jia Z, Liu W. Precise drift tracking for in situ transmission electron microscopy via a thon-ring based sample position measurement. *Microsc Microanal* 2022;28:1945-51. DOI
74. Huang X, Jones T, Fedorov A, et al. Phase coexistence and structural dynamics of redox metal catalysts revealed by operando TEM. *Adv Mater* 2021;33:e2101772. DOI
75. Chen Q, Dwyer C, Sheng G, et al. Imaging beam-sensitive materials by electron microscopy. *Adv Mater* 2020;32:e1907619. DOI